A Computational Workbench Environment for Virtual Power Plant Simulation

Quarterly Progress Report

Reporting Period Start Date: January 1, 2002
Reporting Period End Date: March 31, 2002

Mike Bockelie, REI
Dave Swensen, REI
Martin Denison, REI

April 30, 2002

DOE Cooperative Agreement No: DE-FC26-00NT41047

Reaction Engineering International
77 West 200 South, Suite 210
Salt Lake City, UT 84101

Disclaimer

Abstract

This is the sixth Quarterly Technical Report for DOE Cooperative Agreement No: DE-FC26-00NT41047. The goal of the project is to develop and demonstrate a computational workbench for simulating the performance of Vision 21 Power Plant Systems. Within the last quarter, good progress has been made on the development of our IGCC workbench. Preliminary CFD simulations for single stage and two stage "generic" gasifiers using firing conditions based on the Vision 21 reference configuration have been performed. Work is continuing on implementing an advanced slagging model into the CFD based gasifier model. An investigation into published gasification kinetics has highlighted a wide variance in predicted performance due to the choice of kinetic parameters. A plan has been outlined for developing the reactor models required to simulate the heat transfer and gas clean up equipment downstream of the gasifier. Three models that utilize the CCA software protocol have been integrated into a version of the IGCC workbench. Tests of a CCA implementation of our CFD code into the workbench demonstrated that the CCA CFD module can execute on a geographically remote PC (linked via the Internet) in a manner that is transparent to the user. Software tools to create "walk-through" visualizations of the flow field within a gasifier have been demonstrated.

.

Table of Contents

1

Executive Summary

The work to be conducted in this project received funding from the Department of Energy under Cooperative Agreement No: DE-FC26-00NT41047. This project has a period of performance that started on October 1, 2000 and continues through September 30, 2003.

The goal of the project is to develop and demonstrate a computational workbench for simulating the performance of Vision 21 Power Plant Systems. The Year One effort focused on developing a *prototype workbench* for the DOE Low Emission Boiler System (LEBS) Proof of Concept (POC) design. The Year Two effort is focused on developing a more advanced workbench environment for simulating a gasifier based Vision 21 energyplex.

The main accomplishments during the last three months include:

- Continued discussions with DOE to better define the Vision 21 energyplex reference configuration.
- Preliminary results have been obtained for CFD models of a single stage (down fired) and a two stage (up fired) entrained flow gasifier for operating conditions based on our Vision 21 reference configuration.
- A comparative study of published gasification kinetics has demonstrated that the available kinetics parameters can provide results that vary by several orders of magnitude.
- A strategy has been created for developing the models needed to simulate the equipment and processes downstream of the gasifier in the Vision 21 reference energyplex configuration. Several of these modules will re-use software and sub-models from the prototype workbench developed during Year One of the program.
- A CFD based entrained flow gasifier model has been implemented into a first version of the IGCC workbench.
- Two reactor models and a CFD model that use CCA software protocols have been successfully implemented into a CCA version of the workbench.
- PC based software tools have been developed for creating “walk-through” visualizations that can be used to highlight the complex flow field features in a gasifier. The resulting movies can be replayed using standard Windows based software products.

Each of these topics is discussed in the following sections.

2

Experimental Methods

Within this section we present brief discussions on the many sub-tasks that must be addressed in developing the workbench. For simplicity, the discussion items are presented in the order of the Tasks as outlined in our detailed Work Plan.

Task 1 – Program Management

Two presentations that highlighted material from this project were made at the 27th International Technical Conference on Coal Utilization & Fuel Systems, held March 4-7, 2002 in Clearwater, Florida.

- The first paper, [Bockelie et al., 2002], was presented in a session dedicated to Vision 21 projects and was chaired by the DOE Vision 21 Program Manager. This paper provided an update on the development of our computational workbench including preliminary results for CFD models of downfired and upfired entrained flow gasifiers.
- The second paper, [Swensen et al., 2002], was presented in a Computer Simulation session and highlighted several CFD simulation visualization methods we have developed during the course of this project.

On March 19, 2002 project team members traveled to the EPRI offices in Palo Alto, CA to meet with Dr. Neville Holt, a consultant to this project. The meeting provided us the opportunity to discuss our progress on developing CFD models for entrained flow gasifiers and to discuss publicly available data for use in model development and verification.

Task 2 – Virtual Plant Workbench II

The objective of this task is to demonstrate the capabilities of the computational workbench environment by evaluating the performance of a virtual LEBS power plant. For the many sub-tasks contained under Task 2, the work effort is being performed by software engineers from Reaction Engineering International (REI) and Visual Influence (VI).

The main focus of this sub-task has been to continue to evolve a comprehensive software design, building on the ideas developed for Workbench I. As the complexity and capabilities of Workbench II continue to increase, the software design is evaluated and modified accordingly.

Component Interfaces

As noted in the previous quarterly report, Visual Influence (VI) has delivered to REI an initial version of a CCA framework, which REI engineers then modified to be used within the SCIRun environment. The power of CCA integrated into the workbench was demonstrated, even at this early stage, by executing CCA compliant models residing on geographically distributed computers with little regard to the complexity of the data structures being shared or to any computational resource that the models required.

During the last performance period, REI software engineers have used the SCIRun-based CCA capabilities to incorporate three computational models into the workbench as CCA components. These include an updated SCR, air heater and a *GLACIER* CFD model. (Note that the CCA modules have been implemented into an "alpha" version of Workbench II. During the next quarter the CCA models will be implemented into the current version of Workbench II.)

By far the most complex and computationally intensive of these models is the *GLACIER* CFD model. With run times on the order of days, getting this model functioning as a CCA component has been a high priority. The *GLACIER* module gathers data from the local user interface and sends this data to the remote CCA implementation via the Internet. After calculations are complete, the CCA component sends the resulting data back to the local computer, where the workbench reads the data and then sends out data to other workbench modules as needed, just as if the CFD module had run on the local machine. All of the usual data (gas, plot, and summary data) are returned from this fully functional *GLACIER* CCA model. The communication of model data is performed in a manner that is transparent to the user.

REI personnel continue to interact closely with Visual Influence software engineers regarding CCA capabilities. Visual Influence team members are currently heavily involved in development of the latest CCA specifications and in the implementation of the next generation of CCA software capabilities (through this and other programs). This close working relationship is responsible for not only providing state-of-the-art CCA capabilities to the Vision 21 workbench, but is also contributing to the general development path of CCA, an evolving software protocol for high performance computing applications. The Vision 21 Workbench II is an ideal test bed for the CCA paradigm.

Task 2.2 Visualization

The main focus of this task has been to continue implementing the enhanced visualization capabilities of OpenDX within SCIRun. During the last performance period the ability to create virtual reality based Walk Through presentations of a CFD model was implemented.

Immersive (Walk-Through) Visualization

Traditional visualization techniques require the analyst to be exterior to the data. Immersive environments, such as the CAVE at Argonne National Laboratory or the C-6 at the Iowa State University Virtual Reality Applications Center, provide a more intuitive manner to review model results. Unfortunately, large scale immersive environments are very expensive and require a large physical space to house them. The walk through techniques being developed use OpenDX, require no special hardware and can be utilized by analysts in a typical engineering office.

A walk-through is a virtual reality type of visualization technique that provides the viewer the sensation of flying or walking through the solution domain. When created correctly, this visualization technique can highlight insights into the model predictions that would otherwise not be readily observed. Part of the improved insight is derived from being immersed in the data rather than observing it from a distance. For example, when investigating a burner inlet, one can now guide themselves to a point that gives the best view and then commence building visualizations from that location. This technique gives the analyst a sensation of distance nearly impossible to replicate using traditional visualization techniques. Walk-throughs are currently being developed as either a user guided or a pre-defined-path walk-through. The development of movies described previously has been fully integrated into both user guided and pre-defined-path walk-throughs.

A user guided walk-through is directly supported via OpenDX. The analyst creates a visualization scene and then with the use of the mouse as guidance control moves through the data. Where they go, what they look at, and at what speed they travel is completely determined by the analyst. (Note that many computer games use similar techniques to allow a game-player to move through a scene). This user guided walk-through is the most flexible means for a knowledgeable analyst to explore a solution domain.

A pre-defined-path walk-through is like moving through the solution space on predefined rails. The analyst is now a spectator – the path of the walk-through is guided by a predetermined set of points. The effect of this walk through is very similar to riding a roller coaster through the data. While this technique is more restrictive than a user guided walk-through in pure data analysis, it excels in applications such as: 1) transient data sets, where data changes around the observer as a function of time and 2) defined paths such as streamlines, streaklines or particle paths where the user wishes to observe the solution traveling on a meaningful trajectory. Although not as flexible as the user-guided approach, the pre-defined-path method is a means for non-expert users to make use of walk-through techniques.

The end result of a walk-through in OpenDX is a movie file, which can be converted to virtually any format including MPEG, AVI and Quicktime. These movie file formats can then be viewed on virtually any modern computer using readily available player software.

In the future, walk-through techniques will be expanded to allow the leveraging of stereoscopic visualization techniques developed previously, thus dramatically improving the immersive nature of the visualization. Increasing the definition of a pre-defined-path to include camera orientations would provide not only a smooth transition in location from point to point, but also a smooth transition of camera angles. This would simulate "banking" or "rolls" when traveling through turns.

Task 2.3 Module Implementation/Integration

The focus of this sub-task has been to continue the development of component wrappers needed for Workbench II computational components and to start integrating into the workbench component modules for equipment downstream.

Update on Component Wrappers: Further development has been conducted on component wrappers for the Vision 21 Workbench. At present, skeleton wrappers have been created for all Vision 21 plant components. Upon completion, each of the component wrappers will exist as a fully functional module, which is capable of providing all of the user input, GUI elements and **SCIRun** execution services required by the computational models.

Component Model Integration: Component models for the Syngas Cooler, Recuperator and HRSG have been integrated into the workbench. The component model for the gasifier CFD model (i.e., *GLACIER* steady-state CFD model) using customized C++ wrappers has been completed.

Gasifier Grid Modification: To provide the flexibility to investigate modified gasifier designs, a graphical tool is being implemented into the workbench that will allow the user to easily rescale critical gasifier dimensions. Starting with a computational mesh for a two-stage gasifier, the user is able to choose key points on the units profile and reposition (stretch) them. The repositioning can be performed by (1) selecting and dragging points/ranges with the mouse or (2) inputting exact measurements into data entry boxes. Complete testing of this feature and a similar implementation for the downflow gasifier is in progress.

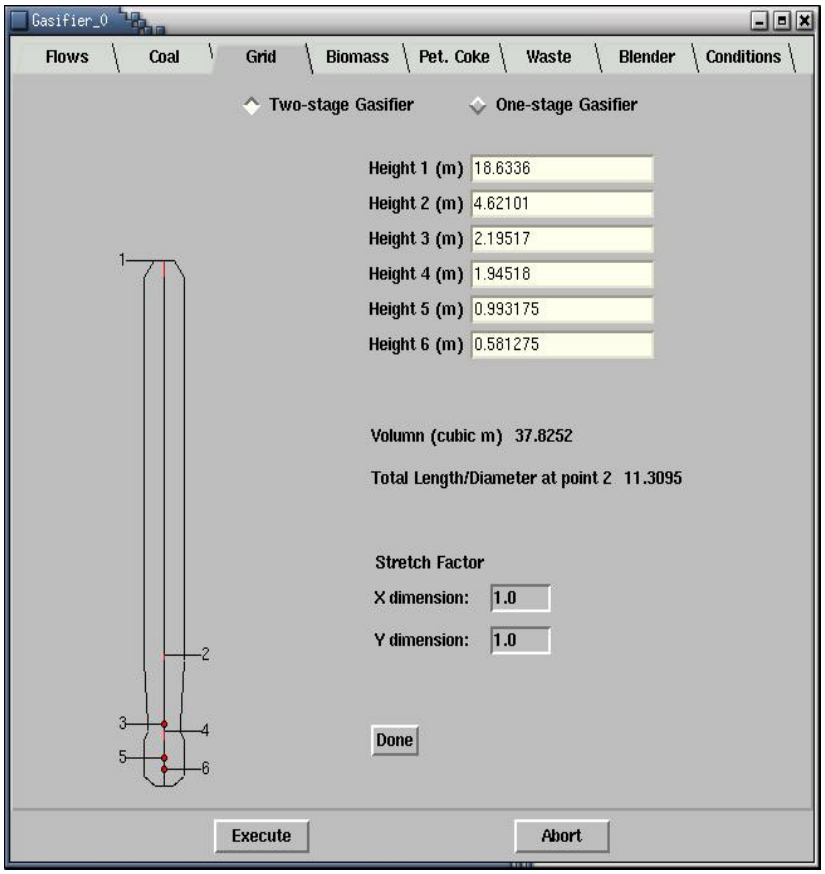

Task 3 – Model Vision 21 Components

The purpose of this task is to develop the reactor and CFD models for the components that will be included in the workbench. In general, these models are first developed in a "stand-alone" form and then subsequently integrated into the workbench environment.

Vision 21 Energy Plex Configuration

Illustrated in Figure 1 is the Vision 21 energyplex configuration that the DOE Vision 21 Program Manager has suggested be used by this project to demonstrate the capabilities of our workbench environment. This configuration consists of an entrained flow gasifier, gas clean up system, gas turbines, heat recovery steam generator, steam turbine and SOFC fuel cells. As described below, a combination of CFD and reactor models will be used to simulate the performance of this configuration. A CFD model will be used for the entrained flow gasifier and simpler models will be used for the remainder of the equipment and processes. As noted below, several of the models for the downstream equipment will be based on models developed for the LEBS-POC prototype workbench developed in Year One of the program.

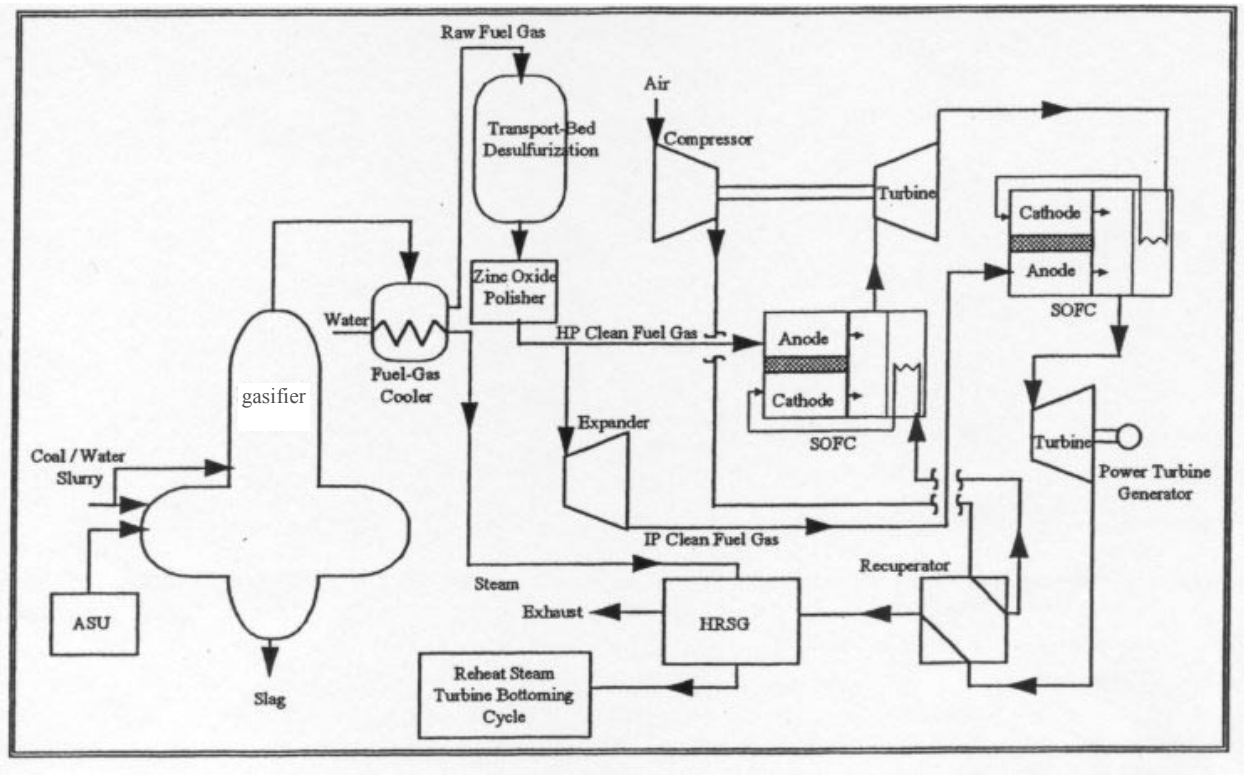

Figure 1. DOE selected Vision 21 test case configuration.

Listed in Table 1 and 2 are the gross conditions for the configuration that were originally provided by DOE.

Table 1. Provided Operating Conditions for Vision 21 Energyplex

Gasifier (15 atm)	Two stage, up-fired
Coal Input to Gasifier (lb/hr)	256,142
Coal Type	Illinois #6
Thermal Input (MW)	875.8
HP SOFC dc/ac	189.4/182.8
LP SOFC dc/ac	121.4/117.2
Gas Turbine, MW	133.7
Steam Turbine, MW	118.0
Fuel Expander, MW	9.6
Gross Power	561.3
Auxiliary Power, MW	40.4
Net Power, MW	520.9
Efficiency, % HHV	59.5

Table 2. Illinois Coal #6 Description

Proximate Analysis	As-Received (wt%)
Moisture	11.12
Ash	9.70
Volatile Matter	34.99
Fixed Carbon	44.19
TOTAL	100.00
HHV (Btu/lb)	11666
Ultimate Analysis	**As-Received (wt%)**
Moisture	11.12
Carbon	63.75
Hydrogen	4.50
Nitrogen	1.25
Sulfur	0.29
Ash	9.70
Oxygen (by difference)	6.88
TOTAL	100.00

Vision 21 Energyplex Configuration - Modifications

Shown in Figure 2 is a mass and energy balance sheet obtained from DOE that provides more detailed information about the targeted Vision 21 configuration. A comparison of Figures 1 and 2 shows some discrepancies. There is important information needed to model the provided system that must be determined. In order to move forward with our project, we have made the following assumptions, based on engineering judgment and information available in the open literature:

- The original data showed no gas recycle from the gas cleanup outflow to the gasifier. Currently our gasifier models do not have this recycle, but we plan to include it once the cleanup models are sufficiently developed.
- We have not been given any information on the steam side conditions for the plant other than steam turbine generator power. We are sizing the steam side assuming double pressure operation at 2400 and 600 psia. The steam temperature to the first stage of the turbine is assumed at 1000 ^{o}F.
- Hot gas cleanup is shown in the data provided by DOE. For warm gas cleanup we will modify the gas cleanup temperature to about 750 ^{o}F by additional syngas cooling between the chlorine guard and the desulferization.
- The operating pressure for the gasifier provided by DOE with Figure 1 (15 atm) would be too low for use with the equipment and conditions shown in Figure 2. Note that a pressure level of 15 atm is the target pressure level for the clean flue gas entering the high pressure fuel cell, which is located well downstream of the gasifier. For our simulations we will assume an operating pressure based on the pressure for the design conditions listed in Figure 2 for the gas clean up equipment immediately downstream of the gasifier (i.e., ~18 atm).

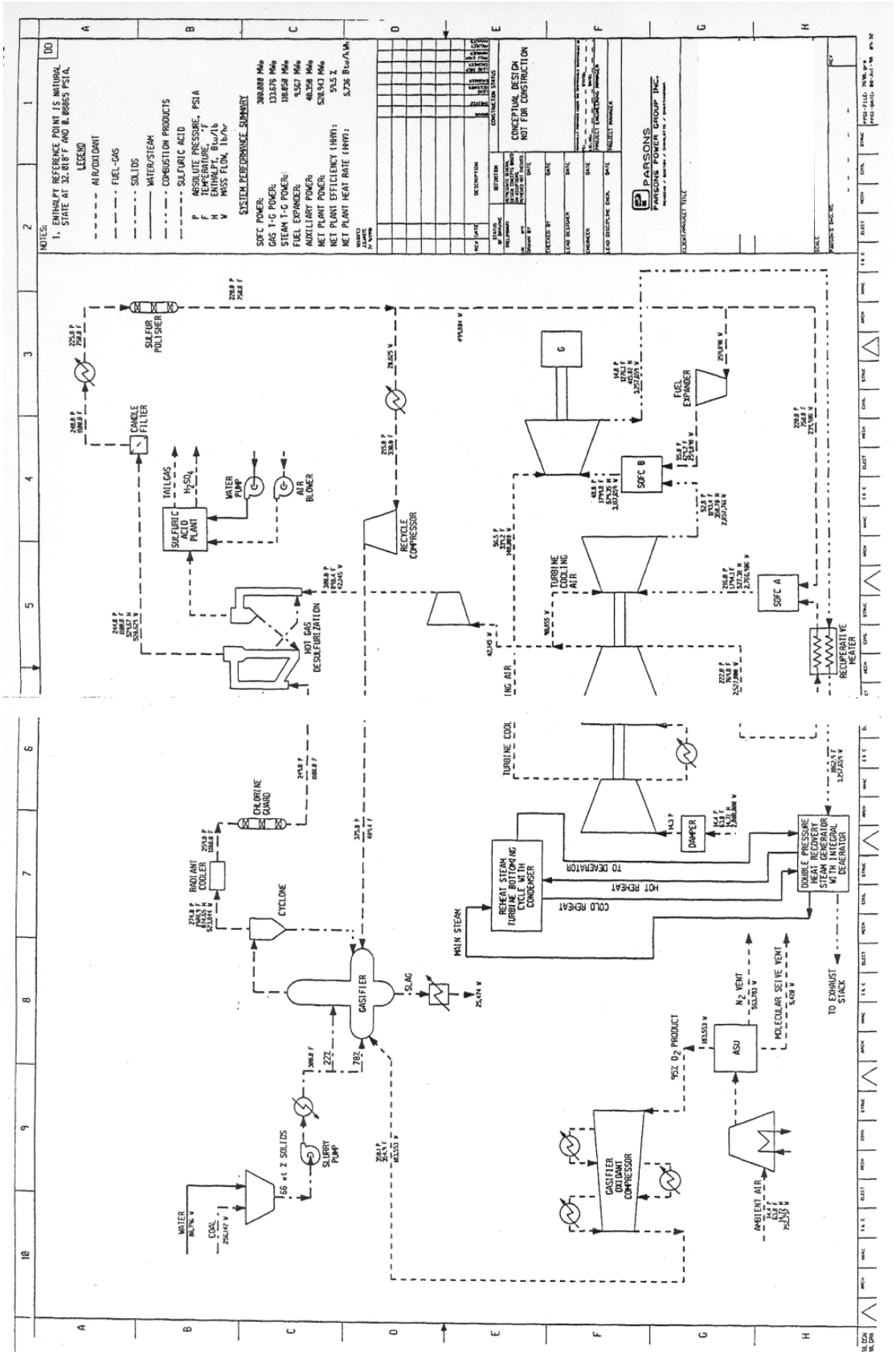

Figure 2. Mass and Energy Balance sheet provided by DOE for Vision 21 reference configuration.

Vision 21 Workbench User Interface

Illustrated in Figure 3 is a SCIRun interface for the Vision 21 reference configuration. Each rectangle in this figure denotes a module (or plant component) with encapsulated functionality. The pipes that connect the modules (or boxes) denote the transfer of model data between modules. Data flows from one component to the next, much in same way that "material" flows through an engineering process flow diagram. Conversion modules are used to allow "data massaging" as the data flows from one component to the next. These are needed because not all models require the same level of detail for their input data (i.e., a module using a detailed CFD simulation is connected to a module using a simple heat/mass balance model). SCIRun provides the flexibility to perform all of the required functions. The inputs for any component model can be inherited from an upstream device or entered directly via input dialog boxes that can contain pull down menus, type-in boxes, radio buttons and menu selections as per standard GUI operation. The visual programming capability within SCIRun allows an engineer to modify the *dataflow network* of the virtual power plant in a user-friendly manner. Additional modules can be instantiated at any time during a computational analysis, as can the connections between modules. The interface to SCIRun can best be described as a graphical programming environment with true plug-and-play functionality.

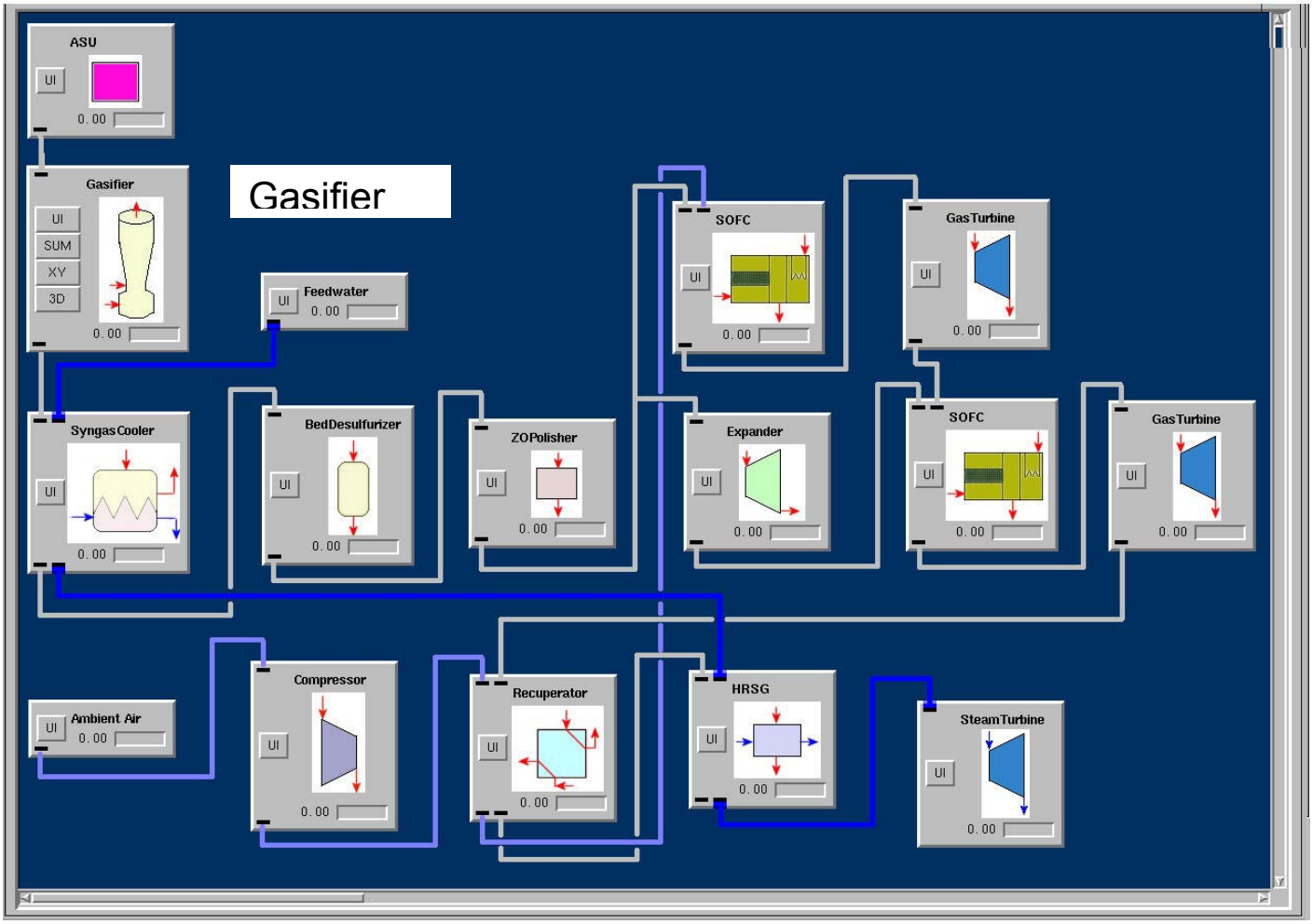

Figure 3. IGCC workbench User Interface for Vision 21 reference configuration.

Task 3.3 Gasifier Models

Good progress has been made on developing CFD based models for entrained flow gasifiers. The models will be created using two different CFD codes. One gasifier model will be developed by REI personnel using *GLACIER*, a comprehensive two phase CFD based reacting CFD code. At present, *GLACIER* is limited to performing steady-state simulations and thus will be used to perform steady state CFD simulations of single and two stage gasifiers. The other gasifier model will be developed by RECOM using *AIOLOS*, a comprehensive reacting CFD code capable of performing transient boiler simulations and thus will be used to perform time dependent simulations for a single stage gasifier. Both CFD codes have been used to analyze numerous coal fired industrial combustion systems. The two codes employ different meshing technologies and different assumptions and sub-models for turbulence-chemistry interaction, simulating two-phase flow and reaction kinetics for combustion and gasification.

Below we highlight the progress within the last performance period in developing the CFD based gasifier models

***GLACIER* Gasifier Module (Steady State):** The *GLACIER* CFD code is a comprehensive CFD modeling code that can be used to model a broad range of turbulent reacting flows. It is capable of modeling two-phase fuels for either gas-particle or gas-liquid applications. For establishing the basic combustion flow field, full equilibrium chemistry is employed. To compute NOx and other trace species, finite rate chemistry effects can be included in a post-processor mode. Turbulence chemistry coupling is accomplished using PDF methods. An important aspect of *GLACIER* is the tight coupling used between the dominant physics for utility boiler applications: turbulent fluid mechanics, radiation heat transfer, chemical reactions and particle/droplet dynamics. Further information on *GLACIER* is available on the web at: http://www.reaction-eng.com/combustion.htm.

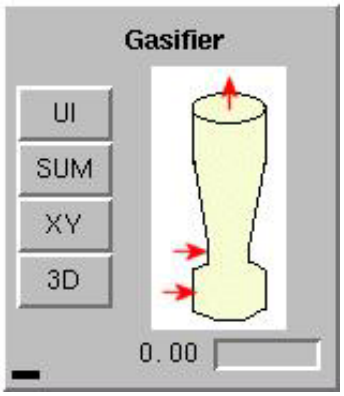

During the last performance period, the development efforts for this model have included incorporating a *GLACIER* based gasifier module into the workbench, creating a User Interface for the *GLACIER* module that is "tuned" for gasifier applications, investigations on published gasification reaction kinetics, further development of a wall slagging model and preliminary model results for a single and two stage gasifier. Details about the model development are described immediately below, whereas further details on the CFD model results are described in the Results and Discussion Section at the end of the report (see page 24).

Model Inputs: Located on the gasifier SCIRun module is a button labeled "UI". Selecting the UI button will cause an input dialog box (see Figure 4) to appear on the screen. Using this window, the engineer can alter the model parameters that impact module performance. The input dialog uses a combination of simple type-in boxes and other standard user-interface elements that request information in terms (and units) typically used in the combustion community.

At present, for the gasifier model the user can modify the coal type and properties, solids ratio of the slurry, flow rates and temperatures for slurry, oxygen and steam and the distributions of slurry, oxygen and steam amongst the injector levels (see Figure 4). Note the detailed information requested for the coal ash properties. This information will be utilized in the slagging model (see below) that is being incorporated into the gasifier model. As described in Section 2.3, a tool to allow the workbench user to modify (in a limited manner) the gross size and shape of the gasifier is being implemented.

To make operation of the workbench as robust and user-friendly as possible, default values are provided for all model inputs where feasible. In addition, all inputs are checked for errors prior to allowing the user to close the dialog. Currently, the provided default values are configured specifically for the Vision 21 reference energyplex (see Figure 1 and Tables 1 and 2). The software design of the user interface allows the provided default values, as well as the input dialog windows, to easily be changed to match alternative designs and to accommodate future model enhancements.

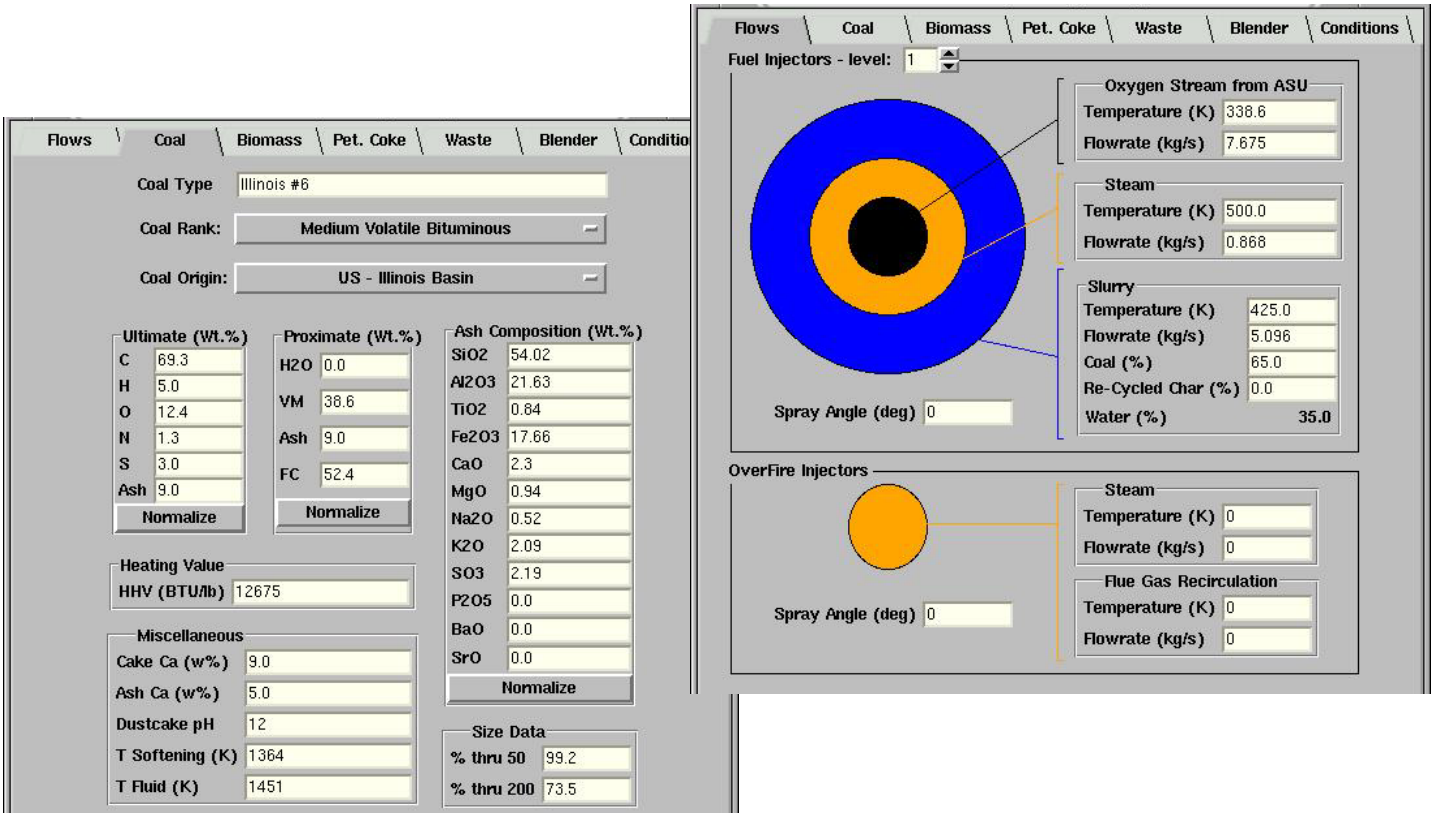

Figure 4. Windows showing gasifier model input panels to enter slurry composition and distribution (upper) and fuel properties (lower).

Model Outputs: A full range of techniques are available for displaying model results (see Figure 5). The most basic form of output is a simple summary table of key values. The tabular output, or summary data, is accessed by clicking on the SUM button on the gasifier module icon and is displayed in a window. Items displayed in the summary data window include average values at the furnace exit for the gas temperature, gas composition (CO, CO_2, CH_4, COS, H_2, H_2O, O_2), carbon conversion (%), average particle residence time and other parameters that describe overall gasifier performance such as total deposition on walls, average fly ash size or possibly the total heat loss by the gasifier. Model output information can also be displayed as XY, or 1D, plots. This information is accessed by selecting the XY button on the gasifier module icon. A variety of information can be plotted, typically weighted average values at a cross-section as a function of axial distance along the reactor. Items available include mass averaged gas field properties such as gas temperature and composition (major species only). In addition, averaged wall properties can be plotted, such as average wall temperature, slag thickness, slag viscosity, etc. Illustrated in Figure 5 is the average gas temperature along the axis of a two stage gasifier. Model output information can also be displayed using 3D visualization methods. The 3D visualization capability is accessed by selecting the "3D" button on the gasifier module icon. The ability to perform standard CFD visualization methods and some low cost virtual reality methods, such as stereoscopic visualization using "stereo glasses", volume rendering and "walk-through" scenarios is being implemented. Shown in Figure 5 is the gas temperature at a selected elevation and several representative coal particle trajectories, colored by volatile content.

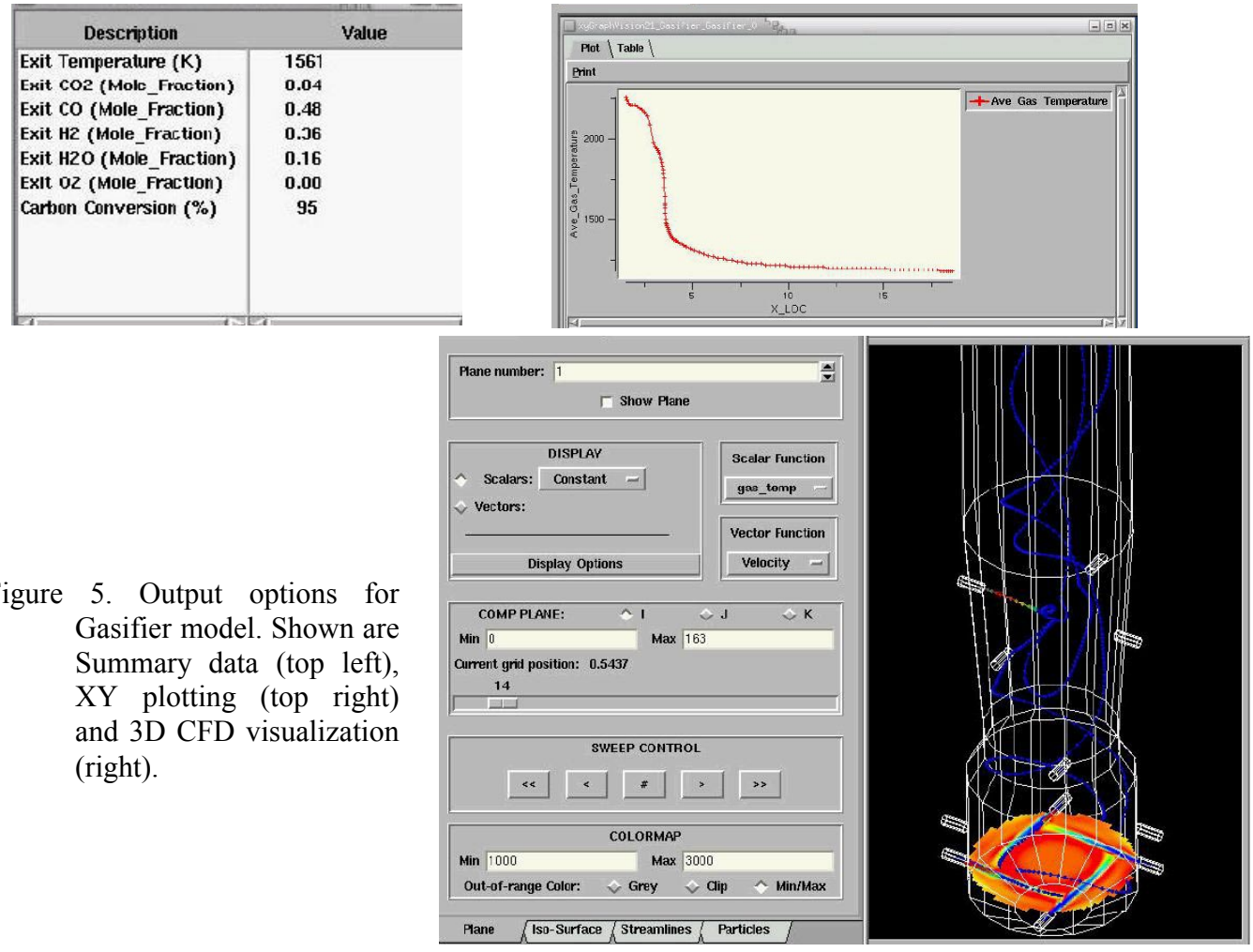

Figure 5. Output options for Gasifier model. Shown are Summary data (top left), XY plotting (top right) and 3D CFD visualization (right).

High Pressure Gasification Kinetics

Having the correct gasification kinetics is critical for any gasifier model. Kinetics are needed to size the gasifier/combustor and determine the char combustion efficiency and possible char recycle requirements. The kinetic parameters need to cover the temperatures and oxygen concentrations along different trajectories within the gasifier, and will therefore be necessary for environments ranging from inert to pure oxygen, temperatures up to 1873 K (2912°F), and pressures of up to 3 MPa (~30 atmospheres). Char gasification by O_2, CO_2, and H_2O is important. Gasification kinetics were drawn from a number of different sources and compared. Emphasis was on kinetics pertinent to entrained flow gasifiers. The kinetics from the literature were also compared with those used in previous models of entrained flow gasifiers. The first set of comparisons were for char reactivity with oxygen.

Five correlations were compared:

1. Banin et al., *Fuel*, **76**, 945-949 (1997) and
   Banin et al., *Combustion and Flame*, **108**, 1-8 (1997)
2. Joutsenoja et al., *Energy and Fuels*, **13**, 130-145 (1999)
3. Monson et al., *Combustion and Flame*, **100**, 669-683 (1995)
4. Lupa and Kliesch, "Simulation of a Texaco Gasifier, Vol.1 A Steady State Model", EPRI Report AF-1179, Vol. 1 Research Project 1037-1. Final Report, 1979
5. Otaka et al., 26th International Conference on Coal Utilization and Fuel Systems, Clearwater, Fl., 2001

Rates were calculated for oxygen concentrations of 1, 10, 30, 100 mole percent, total pressures of 1 to 80 atmospheres, and temperatures of 1400, 1700, and 2000K. The rates can be retarded by combustion products. Hence, the composition of the residual gases was obtained by assuming that the oxygen entrains flue gases - the composition of which was taken from typical values for dry and slurry feed gasifiers (see Table 3 below). In this manner the simulations provide the concentrations that might be expected as oxygen is consumed during reaction starting with its initial value to its final one.

Table 3. Representative Gasifier Product Composition for Dry and Slurry Feed

Component	Dry Coal Feed	H_2O Slurry Feed
H_2	26.7%	30.3%
CO	63.3	38.7
CO_2	1.5	10.8
CH_4	0.0	0.1
H_2S	1.3	1.0
N_2	4.1	0.7
Ar	1.1	0.9
H_2O	2.0	16.5

The rates given by the different correlations ranged over six orders of magnitude. The outlier was the correlation of Monson et al. (1995). A recent presentation by one of the co-authors (T.Fletcher) indicated that they had detected problems with the interpretation of the data and that the values need to be adjusted. We are working on resolving the discrepancies and are

collaborating with Dr. David Harris who is in charge of the char reactivity research at the Collaborative Research Center for Coal and Sustainable Development (CCSD) in Australia. As part of this collaboration we will have access to data being generated in the pilot facility in Pinjarra Hills, Queensland, Australia. In the next quarter, gasification kinetics for CO_2 and H_2O will also be evaluated.

Slagging Model

As described in the last report, we are developing a slagging model that is based on work performed under the High Performance Power Generating System (HIPPS) program [United Technologies Research Center, 1995]. The model uses information from the gas flow field in the gasifier (e.g., gas composition, gas temperature, incident heat transfer, and particle deposition rate) to predict the slag properties (e.g., slag flow, slag thickness, frozen ash thickness) and heat transfer through the walls of the gasifier (for an assumed external ambient temperature).

During the last quarter, we have identified the need to incorporate an ash viscosity submodel into the slagging model. At present, the slagging model uses only a single set of Urbain type equation coefficients and thus the predicted slag viscosity is only a function of temperature. This viscosity model should include the dependence of the Urbain coefficients on ash composition as well as oxidizing versus reducing conditions. We have begun to look at viscosity models that are available in the open literature.

***AIOLOS* Gasifier Module (Transient/Steady State):** The *AIOLOS* CFD code is a comprehensive CFD modeling code that can be used to model a broad range of turbulent reacting flows. It can be used to model two-phase fuel applications, using either Eulerian-Eulerian or Eulerian-Lagrangian methods. *AIOLOS* employs an EDC technique for turbulence chemistry coupling. It can employ multi-domain grids and perform time dependent coal combustion simulations using either implicit or explicit time stepping. It can be used on virtually any level of hardware or operating system. *AIOLOS* is parallel-capable on both SMP and distributed architectures. It can be executed on single or dual cpu PCs/workstations, PC clusters and has been tuned for use on supercomputers. Further information on *AIOLOS* can be found on the web at: http://www.ivd.uni-stuttgart.de/english/aiolos_e_fh.html.

During the last performance period, the development efforts for this model have focused on implementing into *AIOLOS* a sub-model for coal gasification under high pressure and testing the developed model for an idealized single burner simulation. Details about the model development are described immediately below and the CFD modeling results are described in the Results and Discussion Section at the end of the report (see page 24).

It should be noted that at this time the model development efforts for *AIOLOS* are being performed in a "stand alone" mode, or outside of the workbench. The module for the *AIOLOS* based transient gasifier model will not be implemented into the workbench until after completing all model development and testing on selected transient problems.

Implementation of Gasification Chemistry Model into *AIOLOS*

The following paragraphs briefly describe the kinetic model of gasification chemistry implemented into *AIOLOS*, the treatment of turbulence-chemistry interaction in *AIOLOS* and the verification of the correct implementation of the chemistry model.

Kinetic Model of Coal Gasification

The modeling of coal gasification is based on the assumption that the conversion of coal can be divided into three steps. These steps are drying (in case of a wet fuel like biomass or brown coal) and pyrolysis, heterogeneous char reactions and combustion of volatiles. During pyrolysis the coal decomposes to volatile matter and char. The heterogeneous char reactions consider the reactions of char with the gas phase species. For the coal gasification these species are mainly oxygen, steam and carbon dioxide. The third step contains all reactions of the gas phase species. The reaction scheme of the gasification model used in this project is described below by the following reactions.

a) Drying and pyrolysis

{E1}	humid fuel HF	$\rightarrow$	dried fuel DF			(drying)
{E2}	dried fuel DF	$\rightarrow$	volatiles VM	+	char C	(pyrolysis)

b) Heterogeneous reactions:

{F1}	$\phi C + O_2$	$\rightarrow$	$2\bullet(\phi-1)CO + (2-\phi)\ CO_2$	(oxidation of char)
{F2}	$C + H_2O$	$\rightarrow$	$CO + H_2$	(heterogeneous steam reaction)
{F3}	$C + CO_2$	$\rightarrow$	$2\ CO$	(Boudouard reaction)

c) Homogenous reactions:

{G1}	$C_mH_n + m/2\ O_2$	$\rightarrow$	$m\ CO + n/2\ H_2$	(oxidation of hydrocarbons)
{G2}	$C_mH_n + m\ H_2O$	$\rightarrow$	$m\ CO + (m+n/2)\ H_2$	(methane reaction)
{G3}	$CO + H_2O$	$\leftrightarrow$	$CO_2 + H_2$	(homogenous steam reaction)
{G4}	$H_2 + ½\ O_2$	$\leftrightarrow$	H_2O	(oxidation of hydrogen)
{G5}	$CO + ½\ O_2$	$\rightarrow$	CO_2	(oxidation of CO)

These reactions determine the composition of the gas produced and the residual char content depending on the following parameters: total pressure p, temperature T, composition of the fuel (proximate analysis) and the gasification agent (air, oxygen, steam or CO_2) used.

While the residual char content is mainly determined by the heterogeneous reactions, the composition of the produced gas is a function of the very slow homogeneous reactions. This is due to the typically long residence times in gasifiers. Therefore, a reliable gasification model has to consider both sets of reactions. All reactions except {G3} and {G4} are forward reactions. The reaction pathways {G3} and {G4} are considered in the forward and backward directions, which is essential for the accurate prediction of the gas composition. The underlying kinetic rate expressions are summarized in Table 4.

Table 4. Kinetic rate expressions used in *AIOLOS* model

Reac	Kinetic rate	$k_{o,i}$	E_i/R	src
{E1}	$\frac{dw_{FB}}{dt} = -k_{0,F1} \cdot \exp\left(-\frac{E_{F1}}{RT_S}\right) \cdot w_{FB}$	$5.13 \cdot 10^6$ s^{-1}	$1.06 \cdot 10^4$ K	[Chan,1985]
{E2}	$\frac{dw_{TB}}{dt} = -k_{0,F2} \cdot \exp\left(-\frac{E_{F2}}{RT_S}\right) \cdot w_{TB}$	$1.14 \cdot 10^5$ s^{-1}	$8.9 \cdot 10^3$ K	[Norman,1997]
{F1}	$\frac{dw_C}{dt} = -k_{0,F3} \cdot \exp\left(-\frac{E_{F3}}{RT_S}\right) \cdot a_P \cdot w_C \cdot p^*_{O_2}$	$2.08 \cdot 10^2$ (kg/m^2·s·bar)	$9.55 \cdot 10^3$ K	[Norman,1997]
{F2}	$\frac{dw_C}{dt} = -k_{0,F4} \cdot \exp\left(-\frac{E_{F4}}{RT_S}\right) \cdot a_P \cdot w_C \cdot p^*_{H_2O}$	$2.47 \cdot 10^3$ (kg/m^2·s·bar)	$2.10 \cdot 10^4$ K	[Norman,1997]
{F3}	$\frac{dw_C}{dt} = -k_{0,F5} \cdot \exp\left(-\frac{E_{F5}}{RT_S}\right) \cdot a_P \cdot w_C \cdot p^*_{CO_2}$	$2.47 \cdot 10^3$ (kg/m^2·s·bar)	$2.10 \cdot 10^4$ K	[Norman,1997]
{G1}	$\frac{dc_{C_mH_n}}{dt} = -k_{0,G1} \cdot T^{0.5} \cdot \exp\left(-\frac{E_{G1}}{RT_G}\right) \cdot c_{C_mH_n} \cdot c_{O_2}$	$2.33 \cdot 10^{11}$ m^3/(kmol·s·K$^{0.5}$)	$2.01 \cdot 10^4$ K	[Jones,1988]
{G2}	$\frac{dc_{C_mH_n}}{dt} = -k_{0,G2} \cdot \exp\left(-\frac{E_{G2}}{RT_G}\right) \cdot c_{C_mH_n} \cdot c_{H_2O}$	$3.0 \cdot 10^8$ m^3/(kmol·s)	$1.51 \cdot 10^4$ K	[Zimont,1969]
{G3+}	$\frac{dc_{CO}}{dt} = -k_{0,G3} \cdot \exp\left(-\frac{E_{G3}}{RT_G}\right) \cdot c_{CO} \cdot c_{H_2O}$	$2.75 \cdot 10^9$ m^3/(kmol·s)	$1.01 \cdot 10^4$ K	[Zimont,1969]
{G3-}	$\frac{dc_{CO_2}}{dt} = -\frac{k_{0,G3}}{K_{G3}} \cdot \exp\left(-\frac{E_{G3}}{RT_G}\right) \cdot c_{CO_2} \cdot c_{H_2}$	$2.75 \cdot 10^9$ m^3/(kmol·s)	$1.01 \cdot 10^4$ K	[Zimont,1969]
{G4+}	$\frac{dc_{H_2}}{dt} = -\frac{k_{0,G4}}{T_G} \cdot \exp\left(-\frac{E_{G4}}{RT_G}\right) \cdot \frac{c_{O_2}^{2.25} \cdot c_{H_2}^{0.5}}{c_{H_2O}}$	$2.5 \cdot 10^{17}$ m$^{2.25}$·K/(kmol$^{0.75}$·s)	$2.01 \cdot 10^4$ K	[Zimont,1969]
{G4-}	$\frac{dc_{H_2O}}{dt} = -\frac{k_{0,G4}}{T_G \cdot K_{G4}} \cdot \exp\left(-\frac{E_{G4}}{RT_G}\right) \cdot \frac{c_{O_2}^{1.75}}{c_{H_2}^{0.5}}$	$2.5 \cdot 10^{17}$ m$^{2.25}$·K/(kmol$^{0.75}$·s)	$2.01 \cdot 10^4$ K	[Zimont,1969]
{G5}	$\frac{dc_{CO}}{dt} = -k_{0,G5} \cdot \exp\left(-\frac{E_{G5}}{RT}\right) \cdot c_{CO} \cdot c_{O_2}^{0.5} \cdot c_{H_2O}^{0.5}$	$1.3 \cdot 10^{11}$ m^3/(kmol·s)	$1.51 \cdot 10^4$ K	[Howard, 1972]

The quantities in this table are:

- w_j is the concentration of the species j in kg_j/kg_{ges}
- p_j^* is the partial pressure of component j at the particle surface (value is lower the partial pressure in the gas phase due to effects of boundary layer diffusion)
- c_j is the concentration of species j in kmol/m^3
- $k_{0,i}$ and E_i are the pre factor and the activation energy of reaction i
- a_P is the specific particle surface in m^2/kg.

The reactions {G3} and {G4} are evaluated as forward and backward reactions. The corresponding equilibrium constants K_{G3} and K_{G4} are calculated according to [Mueller,1998]:

$$K_{G3} = \frac{c_{CO_2} \cdot c_{H_2}}{c_{CO} \cdot c_{H_2O}} = \exp\left[470.8524 - 175.8711 \cdot (\ln T_G) + 21.95011 \cdot (\ln T_G)^2 - 0.9192934 \cdot (\ln T_G)^3\right]$$

$$K_{G4} = \frac{c_{H_2O}}{c_{H_2} \cdot c_{O_2}^{0.5}} = \exp\left(-6.9793 + \frac{30261.7}{T_G}\right) \text{ in } m^{1.5}/kmol^{0.5}$$

The reaction scheme should be able to predict the gasification process at any pressure level. The heterogeneous reactions consider the partial pressure directly in the corresponding equation. The effect of pressure in the homogeneous reactions is indirectly taken into account by using the unit of kmol/m³ for the concentrations. So each concentration linearly scales with pressure. Nevertheless, it should be noted that the pressure dependence in the heterogeneous reactions is only linear while in the homogeneous reactions the pressure dependence is quadratic.

Heterogeneous Char Reactions

The previously described heterogeneous reaction rates ($k_{0,F1}$ –$k_{0,F3}$) only consider the chemical reaction rate per surface area of the char particles. The effective reaction rate for char reactions though is a combination of the chemical reaction rate k_S and the diffusion rate k_D. So in general the total reduction of char mass can be expressed as:

$$\frac{dw_{Char}}{dt} = -k_{Char} \cdot a_P \cdot w_{Char}$$

where k_{Char} is the effective reaction rate which can be computed by the following equation:

$$k_{Char} = \frac{p_j^*}{\frac{1}{k_S} + \frac{1}{k_D}}.$$

The chemical reaction rate for each char reaction can now be expressed by the following Arrhenius equation with the frequency factor $k_{o,i}$ and the activation energy E_i/R given in Table 4:

$$k_S = k_{0,i} \cdot e^{-(E_i / RT)}$$

For spherical particles the diffusion rate can be calculated by

$$k_D = \frac{24 \cdot Sh \cdot D_j}{R \cdot d \cdot T_{GS}} \cdot 10^5$$

Sh is the Sherwood number and can be set to 2 for spherical particles, D_j is the diffusion coefficient for species j, d is the diameter of the particle and T_{GS} is the boundary layer temperature which can be assumed to be the mean temperature between the particle temperature and the surrounding gas temperature.

The Eddy Dissipation Concept (EDC)

The turbulence-chemistry interaction is modeled using the Eddy Dissipation Concept [Magnusson, 1989] which is a general concept for treating the interaction between turbulence and chemistry in flames. In the EDC the total space is subdivided into a reaction space, the "fine structures" and the "surrounding fluid". All homogeneous reaction are assumed to take place only within these fine structures which can locally be treated as a well stirred reactor transferring mass and energy only to the surrounding fluid. The mean residence time τ_D of fluid within the fine structures is modeled by:

$$\tau_D = 0.41 \cdot \left(\frac{\nu}{\varepsilon} \right)^{0.5}$$

with the dissipation of turbulent kinetic energy ε and the kinematic viscosity ν. The mass fraction γ^* occupied by the fine structures is modeled by:

$$\gamma^* = \left[2.13 \cdot \left(\frac{\nu \cdot \varepsilon}{k^2} \right)^{0.25} \right]^2$$

The reaction rates of all species are calculated on a mass balance for the fine structure reactor. Denoting quantities in the fine structures with an asterisk, the conservation equation of a species j can be written as:

$$\frac{\rho^*}{\tau \cdot (1 - \gamma^*)} \cdot (w_j^* - w_j) = M_j \cdot \omega_j^*$$

in which w_j is the mean mass fraction of species j, w_j^* is the mass fraction of species j within the fine structure, M_j is the molecular weight of species j and ω_j^* denotes the fine structure chemical reaction rate for species j. The mean chemical reaction rate of the species j (ω_j) can then be determined from the chemical reaction rate in the fine structures ω_j^* and the mass fraction of the fine structures γ^*. The presented homogeneous reactions G1 – G5 are modeled as EDC equations and only take place in the fine structures.

Task 3.4 Gas Cleanup and other equipment models

In this sub-task we will develop many of the modules required to simulate the Vision 21 energyplex system. This will include models for the:

- Syngas Cooler
- Heat Recovery Steam Generator
- Gas Recuperator
- SCR
- Turbines, compressors and expanders
- Gas Clean Up
- High and Low Pressure Solid Oxide Fuel Cell

These systems will be modeled with 0D or at most 1D reactor models. Many of these models will be created by re-using models developed as part of the LEBS-POC prototype workbench developed during Year One of the program. Details on the models used in the Year One prototype workbench are available in [Bockelie, 2001]. A brief description of the role of each module for the Vision 21 workbench, our model development plan and current status is described below.

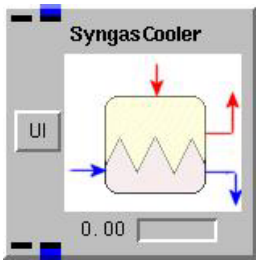

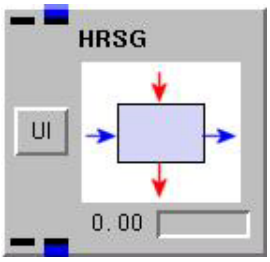

Syngas Cooler and HRSG. The Syngas Cooler and Heat Recovery Steam Generator (HRSG) are heat transfer equipment used downstream of the gasifier that increase the overall thermal efficiency of the energyplex. Models for these systems will be 0D models and will be constructed using the steam heat exchanger models developed in the Year One prototype workbench. We have replaced the previous steam properties module with one based on correlations for the ASME 67 steam tables [McClintock and Silvestri, 1970]. This new steam properties module expands the range of temperature and pressure data and includes entropy needed for the steam turbine thermodynamic calculations. We will provide default inputs (Syngas Cooler and HRSG sizing) consistent with 118 MWe steam turbine generator output. We have completed defining the required steam conditions for this electric output.

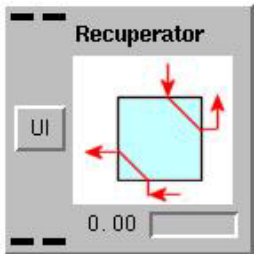

Recuperator. The recuperator is a gas-to-gas heat exchanger used to preheat the compressed air being fed to the high pressure SOFC. The recuperator model will be based on the 0D air preheat heat exchanger model developed for the Year One prototype workbench. We are planning to size this heat exchanger for the specified gas temperatures provided by DOE.

SCR. The data provided by DOE did not include an SCR. Our current SCR model developed in Year One is based on Vanadia/Titania catalysts, which would require placement of the SCR midway in the HRSG for the optimum temperatures.

Steam Turbines. We are planning to incorporate a simple 0D steam turbine model based on thermodynamic calculations using a user input adiabatic efficiency. The efficiency will be applied to an isentropic expansion process using the ASME 67 steam properties module.

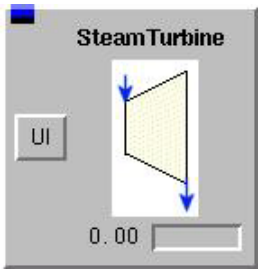

Gas Turbines, Compressors, and Expanders. Similar to the steam turbine model, these models will be 0D models based on thermodynamic calculations and a user input adiabatic efficiency. We will initially assume ideal gas behavior.

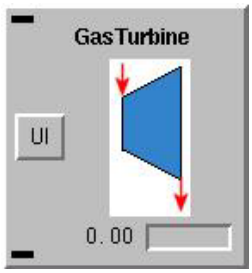

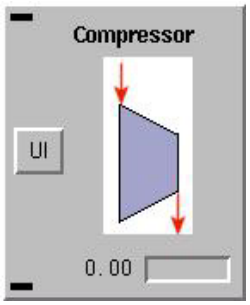

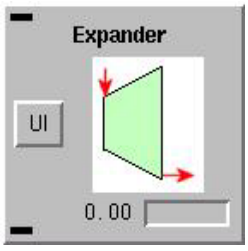

Warm Gas Clean Up. The current generation of gasification systems relies heavily on so-called cold gas clean up systems, which remove particles, acid gases and other trace contaminants at the low temperatures characteristic of conventional power plants and chemical process industry scrubbers. However, DOE has recognized that there is a significant benefit associated with hot gas clean up for gasification systems because of the higher system efficiencies that result when the syngas does not have to be cooled down and reheated before and after the gas clean up process. Several large DOE funded programs have been undertaken to develop hot gas desulfurization systems and hot gas particulate removal systems that would operate at temperatures on the order of 1000 F. Recently, DOE has promoted the use of lower temperatures (500-900 F) for the gas clean up systems, under the umbrella of warm gas clean up systems. Warm gas clean up does not differ in principle from hot gas clean up; at the lower temperatures, new sorbents must be utilized for desulfurization. Such sorbents are currently under development at DOE.

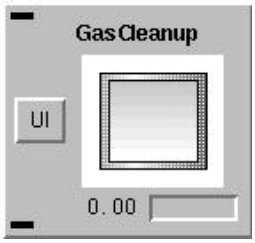

The elements of the gas clean up system can be described in general terms (whether for hot or warm gas clean up). In order to define the system, we assume that the processes that were developed and tested for hot gas clean up can be adapted for warm gas clean up by use of the right sorbents. Figure 6 shows the elements of the warm gas clean up system.

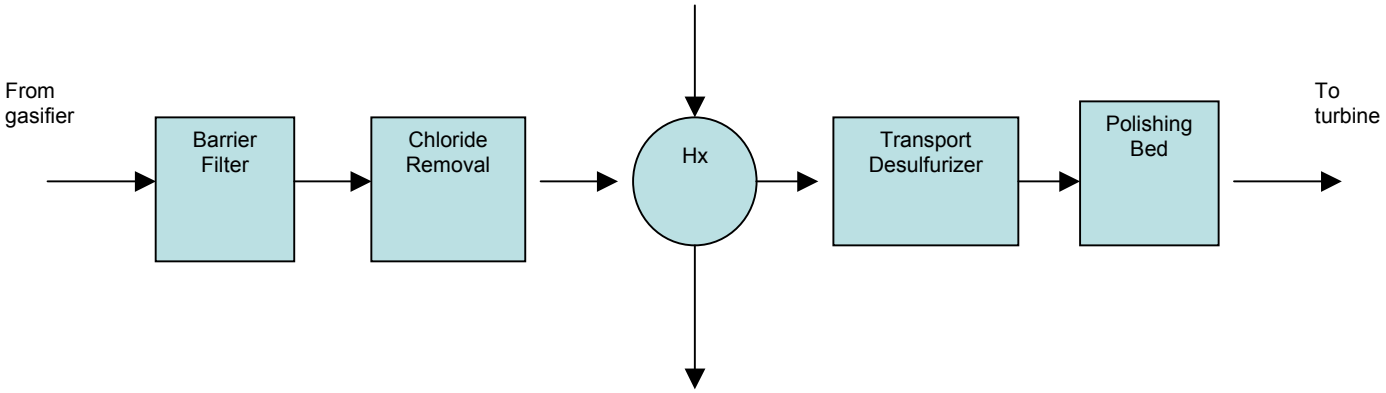

Figure 6. Elements of warm gas clean up system.

Chloride removal is necessary before the sulfur removal step since chloride tends to react with the sulfur sorbents. This also depends on the type of coal gas since some coal gases have higher concentration of chloride. A commercially available nahcolite sorbent operating at 1000 F has been proposed to remove chloride (and other halogens).

For the removal of H_2S and COS, the primary sulfur compounds present in syngas, a regenerable zinc-based sorbent will be used. High temperature sulfur removal using a regenerable metal oxide sorbent uses the following overall reactions (for a given metal M).

Sulfur removal step:

$MO + H_2S = MS + H_2O$ (1)

Sorbent regeneration step:

$MS + O_2 = 3/2\ MO + SO_2$ (2)

The metal used for the sorbent: has a high selectivity for H_2S (and COS) in a practical temperature range; must have the potential (based on thermodynamics) to reduce the sulfur in the raw gas to a low enough level (Table 5); must be stable in both reducing and oxidizing conditions; and must regenerate easily under oxidizing conditions.

Table 5. Sulfur Removal Requirements for Syngas Applications

Application	Total Sulfur (H_2S + COS), ppmv	H_2S Alone, ppmv
Gas Turbine	<20	Not specified
MCFC	0.5	Not specified
PAFC	<50	<20
SOFC	<0.1	Not specified
Chemical production	<0.06	

Research has focused primarily on zinc sorbents, not only ZnO (1), but also more complex mixed metal oxides such as zinc ferrite and zinc titanate. The latter sorbent has been postulated

for use in the transport reactor. RTI [Turk and Gupta, 2001] has done considerable work on a ZnO sorbent (RVS) that can operate at temperatures in the range of 500 F to 1200 F (260 C to 649 C).

The transport reactor, which has been demonstrated for high temperature operation consists of a recirculating system in which the syngas flows co-currently with sorbent in a riser section. A cyclone separates the cleaned syngas from the sorbent and the sorbent falls through a return leg, at the bottom of which it contacts incoming dirty sygas. A portion of the sorbent is removed in the return leg and sent to a regeneration riser. Off-gas from regeneration is processed to produce elemental sulfur or sulfuric acid using conventional technology. Regenerated sorbent is injected back into the riser section of the desulfurization reactor.

The regenerable RVS sorbent, as described in the RTI report can reduce total sulfur in syngas to a level of about 1-2 ppmv using a fixed bed. This will be adequate for gas turbines, but not for chemical production, molten carbonate fuel cells, or solid oxide fuel cells. For this reason, a downstream polishing bed (non-regenerable ZnO) was proposed to reduce sulfur levels down to 60-100 ppbv.

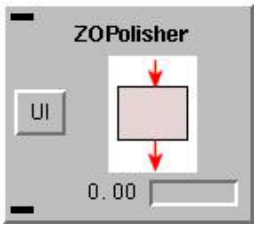

<u>High and Low Pressure Solid Oxide Fuel Cells</u>. We plan to include heat/mass balance reactor models for the high pressure (HP) and low pressure (LP) Solid Oxide Fuel Cell (SOFC). The models will be 0D, mass energy balance models for simple geometric configurations that exhibit the important fluid dynamics, heat transfer, chemical and electrochemical reactions, species transport, etc. The SOFC models will provide a simple test platform to understand the gross effects for SOFC cells. More accurate models could be developed, but would require resources beyond that available in this project. Preliminary discussions have been held with the National Fuel Cell Research Center (NFCRC) at the University of California, Irvine

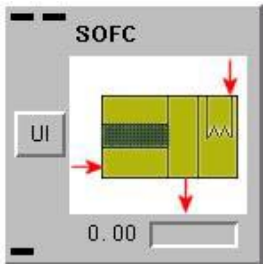

Results and Discussion

During the last quarter we have placed a heavy emphasis on developing CFD models for the entrained flow gasifier models. Described below are preliminary CFD modeling results.

Preliminary Model Results – *GLACIER* Gasifier Model

CFD calculations using *GLACIER* have been performed to simulate gasification behavior in "generic" single stage (down-fired) and two stage (up-fired) pressurized, entrained flow gasifiers (see Figure 7). The geometry of the two gasifiers has been determined using a combination of publicly available information (e.g., engineering articles, advertising literature and web pages) and engineering judgment. The internal shape of the down-fired gasifier is based on information described in [Schneyer et al., 1982] for a pilot scale facility. The shape of the two stage (upflow) gasifier is based on information contained in a series of articles by Chen et al. [Chen et al., 1999], [Chen et al., 2000] that describe modeling studies and scale-up for a pressurized, air blown entrained flow gasifier designed to operate at 2000 tpd of coal. Additional assumptions used to determine the size of the gasifiers were (1) the gasifiers should provide about a two second residence time for the gases (assuming idealized flow) and (2) the length to diameter ratio (L/D) for the single and two stage gasifier are, respectively, approximately two and ten. For the single stage gasifier, the length L is the length of the main chamber and the diameter D is the internal diameter of the refractory surface. For the two stage gasifier, the length L is based only on the vertical riser section (of constant diameter) and D is the internal diameter of the riser; the dimensions of the combustion chamber at the bottom of the gasifier were obtained by scaling the information contained in the articles by Chen et al.

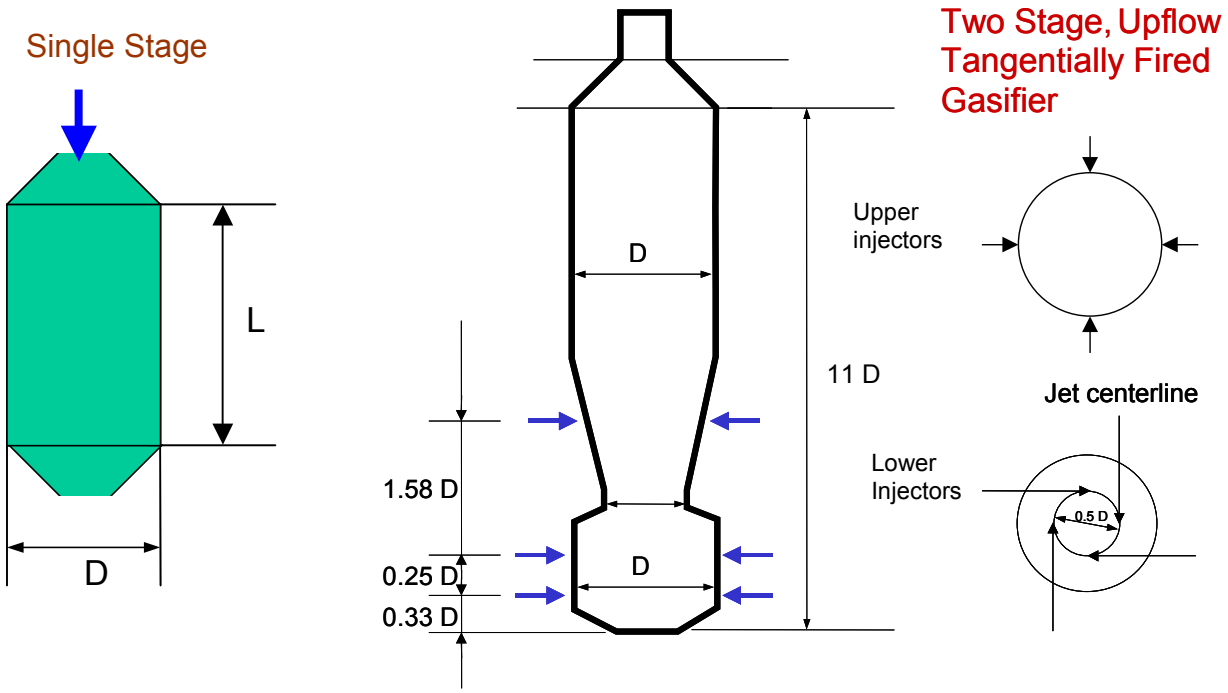

Figure 7. Schematics for single and two stage generic gasifiers used in simulations.

The single stage gasifier contains a single, central nozzle located at the top of the reactor through which the oxygen, steam and coal-water slurry mixture are injected into the gasifier. The burner is assumed to be an double annulus burner with oxygen passing down a center passage, a slipstream of stream is located in the first concentric annulus and the slurry passes through the outer concentric annulus. The annular passages are oriented toward the injector centerline (at the injector tip) and thus result in a spray entering into the gasifier. The injector inlet is scaled to have an injection velocity of about 125m/s for the slurry.

The two stage gasifier contains three levels of symmetrically placed injectors. Here, the fuel injectors are assumed to have a simple annular passage (concentric pipes) that do not produce a spray action. The bottom two levels of injectors are oriented as per a tangential firing system to create a strong swirling flow field that spirals upward along the axis of the gasifier. The upper level of injectors are oriented opposed to each other.

The operating conditions used for the simulations are based on the information provided for the Vision 21 reference configuration (see Tables 1 and 2). The fuel feed is 3000 tpd of Illinois #6 coal, a slurry composition that is 65% solids by weight (a H_2O:coal ratio of about 0.32) and an O_2:coal ratio of about 0.58. For the single stage gasifier all fuel and oxidizer enter through a single injector as described above. For the two stage gasifier, 2/3 of the coal and all of the oxygen is injected through the injectors in the bottom two levels. The coal and oxygen are uniformly distributed amongst the injectors in the two lowest levels. The remainder of the coal is injected at the upper level injectors (uniformly distributed). For these simulations, it was assumed the gasifier operates at 15 atmospheres. Kinetic parameters for coal combustion and gasification have been taken from [Lupa and Kliesch, 1979].

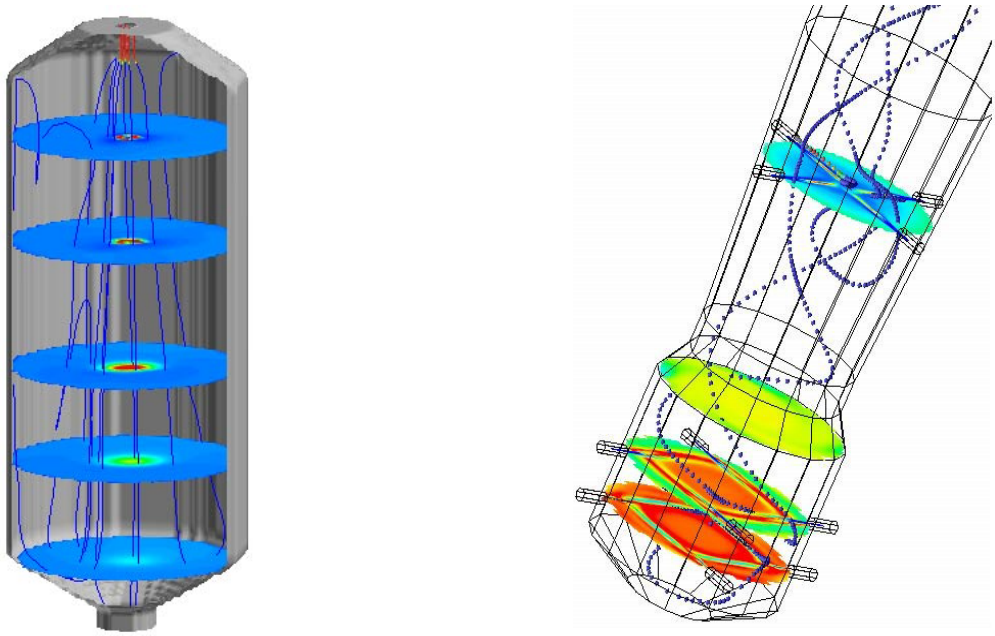

Figure 8. Gas temperature at selected elevations and selected coal cloud particle trajectories for an entrained flow single stage gasifier (left) and two stage gasifier (right). The gas temperature color map uses blue for cool gas (1000K) and red for hot gas (2500K). The particle trajectories are colored by percentage of coal volatile content, with red corresponding to 100% volatiles remaining and blue implying 0% of the coal volatiles remain.

Illustrated in Figure 8 are sample modeling results for the CFD modeling studies. Shown in Figure 8 are the predicted gas temperature at selected elevations and the coal particle trajectory, colored by coal volatile content, for selected trajectories. To simplify plotting, only the lower half of the two stage gasifier is shown in Figure 8.

- In the single stage gasifier, it can be seen that the hot gases remain near the centerline of the reactor, with large regions of cool gas located at the walls. A plot of the velocity field would show high velocity gas moving down the centerline of the vessel, with very low velocity gas moving in the reverse direction (i.e., recirculating flow) everywhere away from the centerline region. It should be emphasized that the flowfield is not a plug flow reactor with a uniform flow nor is the flow field "fully-mixed".

- In the two stage gasifier, as expected, a strong swirling flow pattern along the axis of the gasifier can be seen in both the gas flow field and the particle trajectories. For this gasifier, there is sufficient oxygen available in the bottom section of the gasifier to obtain gas temperatures comparable to those of an oxygen enriched combustion process. In the upper region of the reactor, the gases are much cooler.

- In both simulations, nearly symmetric flow field patterns are observed.

Illustrated in Figure 9 are the mass averaged values for the gas temperature and major gas species along the axis of the two gasifiers. From these plots the differences in the syngas generation process in the two reactors can be seen.

- In the single stage (downfired) gasifier, away from the fuel injector the gas temperature increases until reaching a peak about 60% of the way down the reactor, after which the temperature decreases due to the endothermic reactions in the gas-water shift. In addition, the competition between the different reactions can be observed in the plots of gas composition.

- In the two stage (upflow) gasifier the changes in gas temperature and gas concentration have an asymptotic type of behavior. The sharp wiggles in these plots at the 4m elevation corresponds to the location of the upper injectors.

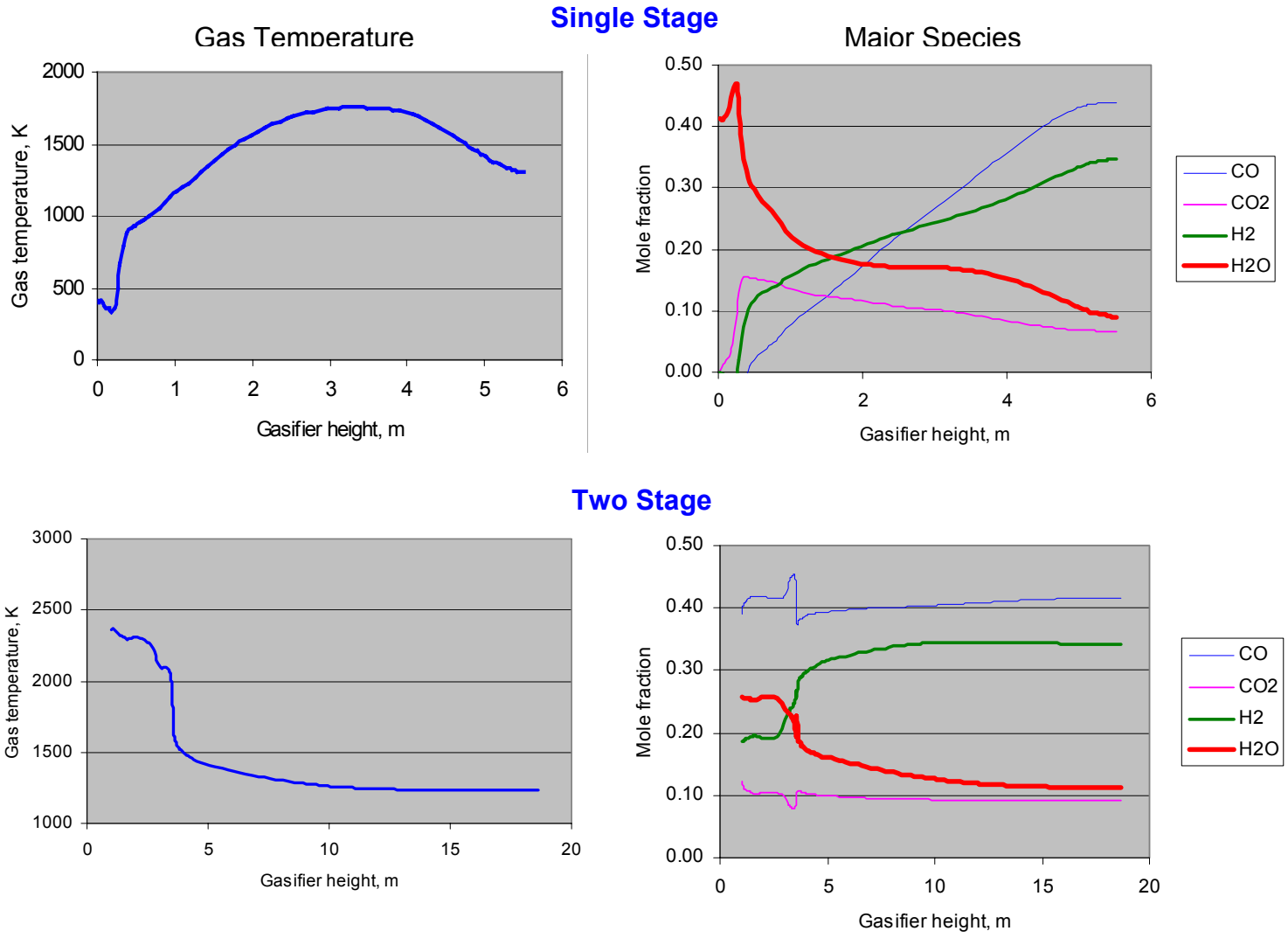

Figure 9. Mass average values for gas temperature and major species along axis of gasifier. The upper row of figures shows results for the single stage (downfired) gasifier and the lower row of figures shows the results for the two stage (upflow) gasifier.

Shown in Table 6 below are the average values at the exit of the gasifiers. Overall, the gasifiers provide approximately the same performance with respect to syngas composition and temperature and carbon conversion.

Table 6. Summary of values at gasifier exit

	Downfired	Upfired
Gas Temperature (K)	1300	1230
CO (vol %)	44	42
CO2 (vol %)	7	9
H2 (vol %)	35	34
H2O (vol %)	9	11
Other (vol %)	5	4
Coal Burnout (mass %)	97	85
Ave. residence time of particles exiting gasifier (sec.)	<0.1	~0.1

It should be emphasized that the modeling results presented here are very preliminary and in no way indicate that one gasifier design is "better" than the other. As described in the work effort summary contained in Task 3.3 (Gasifier Models), many improvements need to be incorporated into the models. In addition, the size and operating conditions used in these simulations may not be optimal for the gasifier designs employed.

Preliminary Calculations - *AIOLOS*

The proposed kinetic gasification model was implemented into the 3D furnace simulation code *AIOLOS*. Since the definition of a suitable gasifier geometry together with corresponding operational parameters for validation purposes is still in progress, the implemented gasification model was verified in a first step on a coal burner test case under combustion conditions. The simulation results of the gasification model were compared to the results of the standard EDC combustion model. The simulation results for the gasification model shows a slightly higher temperature level in the recirculation zone of the coal burner, Figure 10. This can be attributed to the slightly increased char combustion rates predicted by the gasification chemistry model in that region (see Figure 11). Figure 12 shows similar carbon monoxide distributions for the standard EDC combustion model and the new gasification model.

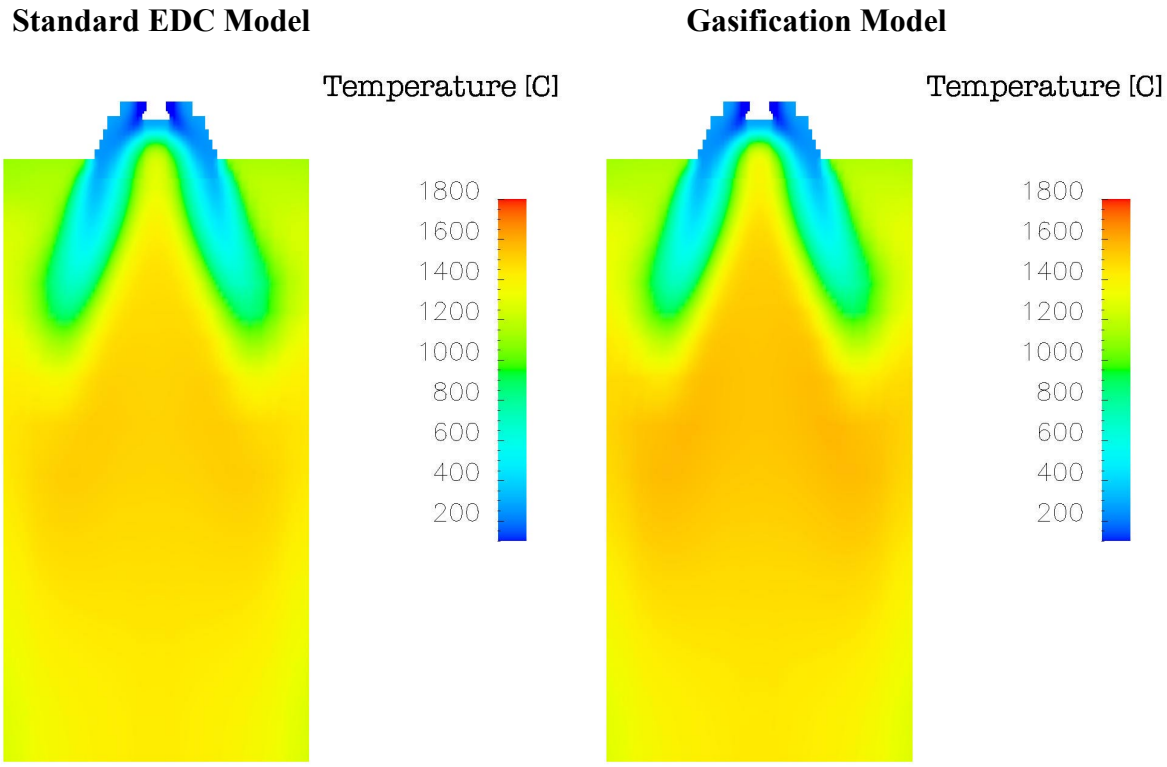

Figure 10. Temperature distribution

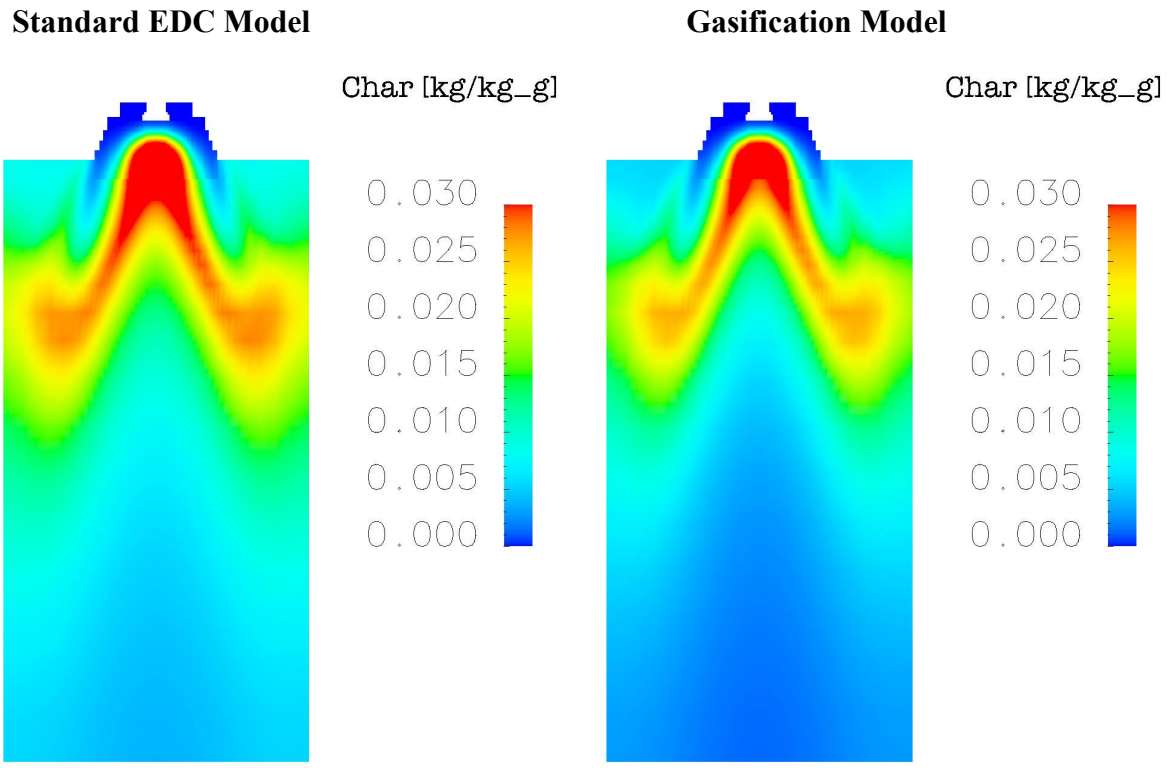

Figure 11. Char distribution

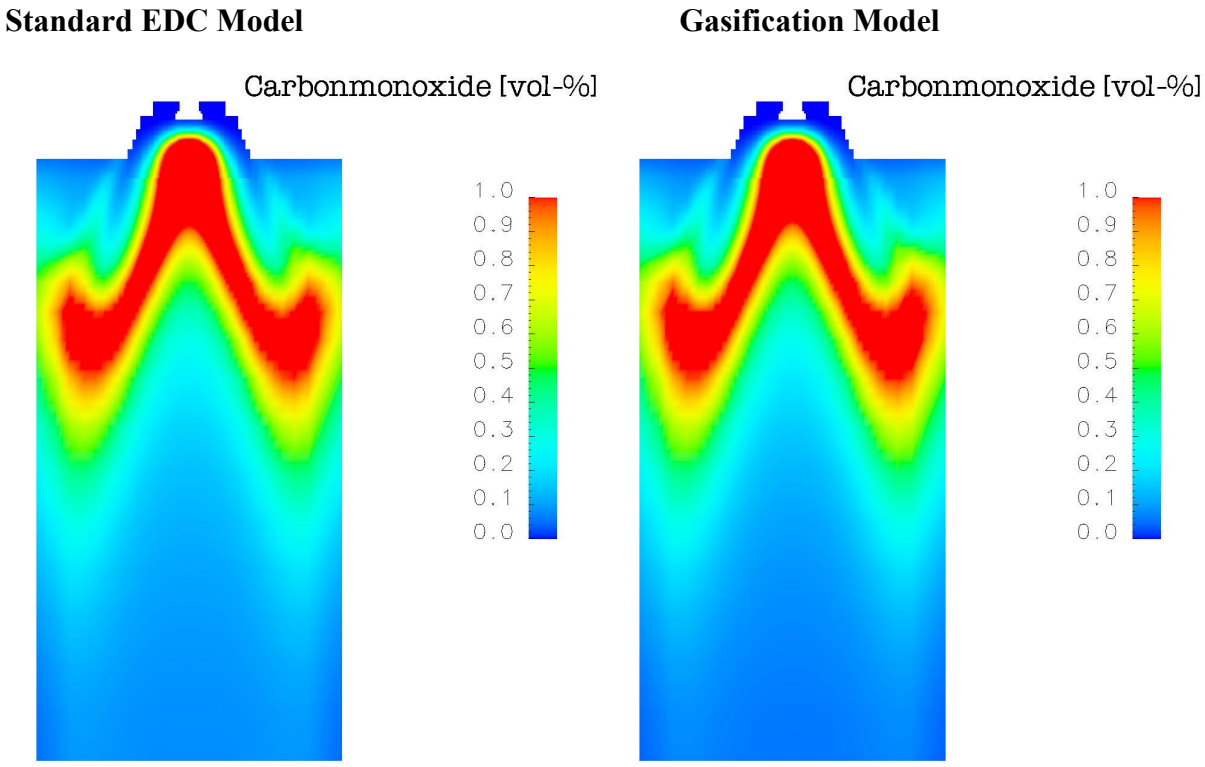

Figure 12. Carbon Monoxide distribution

Conclusions

During the last quarter good progress has been made on the development of our IGCC workbench. Preliminary CFD simulations for single stage and two stage "generic" gasifiers using firing conditions based on the Vision 21 reference configuration have been performed. A plan has been outlined for developing the reactor models required to simulate the heat transfer and gas clean up equipment downstream of the gasifier. Three models that utilize the CCA protocol have been integrated into an "alpha" version of the workbench. Tests of a CCA implementation of our CFD code into the workbench demonstrated that the CCA CFD module executes on a geographically remote PC (linked via the Internet) in a manner that is transparent to the user. Last, visualization tools to create "walk-through" visualizations of the flow field within a gasifier have been demonstrated.

Plans for the next quarter include: further development of the CFD gasifier models, with special focus on reaction kinetics, incorporating the slagging sub-model into the CFD code and detailed modeling studies of a fuel injector; developing models required to model equipment downstream of the gasifier for the energyplex reference configuration; and implementing modifications to the workbench software infrastructure to support further development of the IGCC workbench, such as the gasifier modification tool and completing the CCA implementation of the CFD gasifier model.

References

Bockelie, M.J., Swensen, D.A., Denison, M.K., Sarofim, A.F., "A Computational Workbench Environment For Virtual Power Plant Simulation," presented at the Vision 21 Program Review Conference, Morgantown, WV, Nov. 6-7, 2001.

Bockelie, M.J., Swensen, D.A., Denison, M.K., Chen, Z., Senior, C.L., Sarofim, A.F., "A Computational Workbench Environment for Virtual Power Plant Simulation", *Proceedings of the 27th International Technical Conference on Coal Utilization and Fuel Systems*, Clearwater, FL, USA, March 4-7, 2002.

Chan, W.R.; Kelbon, M.; Krieger, B.B.: "Modelling and Experimental Verification of Physical and Chemical Processes During Pyrolysis of a Large Biomass Particle", FUEL, Vol. 64, pp. 1505-1513, 1985.

Chen, C. Miyoshi, T., Kamiya, H., Horio, M., and Kojima, T., "On the Scaling-up of a Two-Stage Air Blown Entrained Flow Coal Gasifier", The Canadian Journal of Chemical Engineering, **77**, 745-750 (1999).

Chen, C., Horio, M., and Kojima, T., "Numerical Simulation of Entrained Flow Coal Gasifiers", Chemical Engineering Science, **55,** 3861-3883 (2000).

Howard, J.B., Williams, G.C., Fine, D.H.: "Kinetics of Carbon Monoxide Oxidation in Post-Flame Gases", 14th Symposium (International) on Combustion, The Combustion Institute, Pittsburgh, PA, pp. 975-986, 1972.

Jones, W.J.; Lindstedt, R.P.: "Global scheme for hydrocarbon combustion", Combustion and Flame, Vol. 73, p. 233, 1988.

Lupa, A.J. and Kliesch, H.C., "Simulation of a Texaco gasifier, Volume 1: A steady-state model," EPRI final report, September 1979.

Magnussen, B.F: "The Eddy Dissipation Concept", XI Task Leaders Meeting – Energy Conversion in Combustion, IEA, 1989 .

Marion, C.P. and Reynolds, B., "Synthesis gas generation," U.S. Patent 3,705,108, 1972.

McClintock, R.B. and Silvestri, G.J., "Some Improved Steam Property Calculation Procedures," Journal of Engineering for Power, April 1970.

Mueller, C.: 'Numerische Simulation industrieller Verbrennungsprozesse unter Verwendung von reaktionskinetischen Ansätzen und Wirbelszerfallsmodellen', Dissertation, Universität Bochum, 1998.

Norman, J.; Pourkashanian, M.; Williams, A.: "Modelling the formation and emissions of environmentally unfriendly coal species in some gasification processes", FUEL, Vol. 76, No. 13, 1997.

Schneyer, G.P., Cook, J.L., Brownell, D.H.,Jr. and Blake, T.R., "Dynamic simulation of a single-stage entrained flow coal gasifier," EPRI final report, December, 1982.

Swensen, D.A., Maguire, M., Spencer, R., Shino, D., Li, X., Bockelie, M.J., "Visualization Techniques for CFD Simulations of Industrial Systems", presented at the 27th International Technical Conference on Coal Utilization and Fuel Systems, Clearwater, FL, USA, March 4-7, 2002.

Turk, B.S. and Gupta, R.P., *Development and Experimental Results on RVS-1 Dsulfurization Sorbent*, Topical Report to US DOE on Contract DE-AC21-88MC25006, March 2001.

United Technologies Research Center, "Coal-Fired High Performance Power Generating System," Final Report DE-AC22-92PC91155, August, 1995.

Zimont, V.L., Trushin, Y.M.: 'Total Combustion Kinetics of Hydrocarbon Fuels', Comb. Explosion and Shock Waves, Vol. 5, No. 4, pp. 391-394, 1969.